



# EFFECT OF BASE PARAMETERS ON THE GATE-CONTROLLED SQUEEZE OF A CURRENT-CONDUCTING REGION IN *pnpn* STRUCTURES

Z. S. GRIBNIKOV<sup>1</sup>, A. N. KORSHAK<sup>1</sup>, N. Z. VAGIDOV<sup>1</sup> and V. V. MITIN<sup>2</sup>

<sup>1</sup>Institute of Semiconductor Physics, Ukrainian National Academy of Sciences, Kiev 252650, Ukraine and

<sup>2</sup>Department of Electrical and Computer Engineering, Wayne State University, Detroit, MI 48202, U.S.A.

(Received 24 February 1995; in revised form 15 August 1995)

**Abstract**—If a gate current is smaller than some critical value required for the complete turn-off of an anode current in a  $p^+nnpn^+$ -structure it produces the stationary squeeze of current-conducting region (CCR) and increase of the current density in it. The process of squeezing depends on a longitudinal conductivity of the controlling  $p$ -base which is electrically-connected with the gates. But the conductivity along the controlled  $n$ -base which is not connected with the gates affects the process of squeezing indirectly as well. This effect takes place mainly due to the current bias of a parasitic transistor which is formed in a depletion region of the structure and divides the substantial part of the gate current. Calculations of the CCR squeeze which take into account base conductivities are described in this work.

## NOTATION

$e$	magnitude of electron charge
$k_B$	Boltzmann's constant
$T^*$	temperature
$T$	$= k_B T^*$ , temperature in energetic units
$\tau_{p,n}$	lifetimes of carriers in $p, n$ -bases
$y$	coordinate in plane of $p$ - $n$ -junction perpendicular to device strip
$l$	half-width of device strip
$\eta$	$= y/l$ , dimensionless coordinate
$w_{p,n}$	thicknesses of $p, n$ -bases
$x_c$	width of CCR
$L_{p,n}$	diffusion lengths in $p, n$ -bases
$\alpha_{p,n}$	transport factors of $p, n$ -bases
$\gamma_{p,n}$	$= \alpha_{p,n}/(1 - \alpha_{p,n})$
$\varphi$	voltage across device
$\psi$	$= e\varphi/T$ , dimensionless voltage across device
$\varphi_{p,n}$	potentials in $p, n$ -bases
$\psi_{p,n}$	$= e\varphi_{p,n}/T$ , dimensionless potentials in $p, n$ -bases
$N_{p,n}$	hole, electron concentrations
$\mu_{p,n}$	hole, electron mobilities
$\sigma_{p,n}$	$= eN_{p,n}\mu_{p,n}$ , sheet conductivities of $p, n$ -bases
$\xi$	$= \sigma_n/\sigma_p$
$J_a$	anode current
$\Lambda_a$	$= eJ_a l/2\sigma_p T$ , dimensionless anode current
$J_g$	gate current
$J_{g1}, J_{g2}$	gate current components
$\Lambda_g$	$= eJ_g l/2\sigma_p T$ , dimensionless gate current
$\Lambda_M(\Lambda_a)$	maximum value of $\Lambda_g$ which maintains state of maximum squeezing
$j_{a,c}$	anode, cathode current densities
$\bar{j}_a$	mean anode current density
$\lambda_{a,c}$	$= j_{a,c}/\bar{j}_a$ , dimensionless anode and cathode current densities
$K_g$	$= \Lambda_g/\Lambda_M(\Lambda_a)$ , thyristor gate gain
$n_0, p_0$	equilibrium concentrations of minority carriers
$\beta_{p,n}^2$	is determined by eqn (4)
$\kappa^2$	$= (\beta_p)^2/(\beta_n)^2$

## 1. INTRODUCTION

With this work we continue to study an effect of the stationary squeezing of the current-conducting region (CCR) in the  $p^+nnpn^+$ -structure which is in the ON-state with the large current. The squeeze of the CCR is caused by the gate turning-off current which is insufficient to turn off the given anode current  $J_a$  completely. (The current  $J_a$  is given per unit length of the device cathode which is similar to a long strip.)

The regime of the stationary squeeze of the CCR[1] which can be named as the regime of incomplete turn-off (RITO) of the  $p^+nnpn^+$ -structure can be convenient for controllable light-emitting devices including both incoherent light emitters and injection lasers. (It was noted in Ref.[2].) Here we keep all assumptions and approximations which were claimed in our previous article[3]. Namely, we assume that the thicknesses of both middle bases  $w_{n,p}$  in the  $p^+nnpn^+$ -structure are small in comparison with the half-width  $l$  of the device strip:

$$w_{n,p} \ll l \quad (1)$$

and a low-injection condition is realized in both bases for the interesting current and squeeze ranges. That is we assume that a linear recombination regime takes place. Besides, let us assume that the quasi-one-dimensional approach which was applied in Ref.[3] for the calculations of diffusion currents in  $pn$ -junctions remains valid here. (Of course, this quasi-one-dimensional approach does not mean one-dimensionality of distributions of potentials and current densities which are substantially two-dimensional.)

But in contrast to Ref.[3] the basic system of two continuity equations in the middle bases is solved precisely for an arbitrary ratio of longitudinal conductivities  $\xi = \sigma_n/\sigma_p$ . Here  $\sigma_n$  and  $\sigma_p$  are sheet conductivities of the  $n$ - and  $p$ -bases, respectively; for example,  $\sigma_n = eN_n\mu_n w_n$ , where  $N_n$ ,  $\mu_n$  are an electron concentration and mobility in the  $n$ -base;  $\sigma_p$  can be introduced analogously. In the case of very low conductivity of the controlled  $n$ -base  $\sigma_n$  in comparison with the conductivity of the controlling  $p$ -base  $\sigma_p$  (i.e.  $\xi \ll 1$ ) the problem was reduced to a single differential equation[3].

The system of continuity equations allows us to obtain distributions of potentials  $\varphi_{n,p}(y)$  in the middle bases ( $y$ -axis is perpendicular to the device strip in the plane of the  $pn$ -junction, see Fig. 1). When  $\varphi_p(y)$  and  $\varphi_n(y)$  are found we can calculate distributions of anode and cathode current densities  $j_a(y)$  and  $j_c(y)$ ,  $|y| \leq l$ . We assume that the  $p$ -base is the controlling base with the gate contacts and  $n$ -base is the controlled base without them (see Fig. 1).

Distributions of the current densities  $j_{a,c}(y)$  are inhomogeneous in the RITO: in the middle of the device strip  $|y| \leq x_c$  (Fig. 1) the CCR appears. This region is in the ON-state and all three  $pn$ -junctions are forward-biased. The cathode current density  $j_c(y)$  differs from the anode current density  $j_a(y)$  by very little (i.e.  $j_c(y) \simeq j_a(y)$ , for  $|y| \leq x_c$ ). It is disrupted at the edge of the CCR where a part of the anode current divides along the  $p$ -base into the gate. It is one of the gate current components  $J_{g1}$ . Just this component determines width  $2x_c$  of the CCR and current density  $j_a \simeq J_a/2x_c$  in it. Current  $J_{g1}$  is formed in some intermediate region. In this region the forward bias of the middle junction 2 at first and the forward bias of the cathode junction 1 afterwards are changed by reverse biases. Therefore current  $J_{g1}$  flows into the gate along the channel which is insulated by depletion layers of the reverse-biased junctions 1 and 2 on both sides. The anode junction 3 continues to stay in the forward-biased state everywhere. Together with the reverse-biased junction 2 it forms a  $p^+np$ -transistor outside the CCR. The collector current of this transistor is the second component of the gate current  $J_{g2}$ . The component  $J_{g2}$  is a parasitic one since it does not control the CCR squeeze directly in contrast to  $J_{g1}$ . In the case  $\xi = 0$  the above mentioned parasitic  $p^+np$ -transistor (PT) operates with zero base current which is in a floating base regime. But

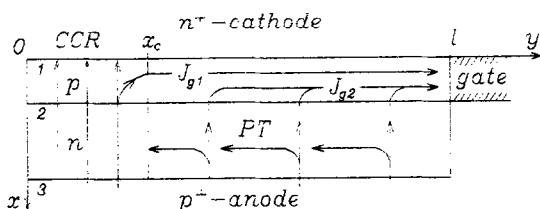


Fig. 1. Division of the current in the  $p^+npn^+$ -structure in the RITO. The right half of the device strip is shown.

if the controlled base conductivity  $\sigma_n$  is distinct from zero the CCR biases the PT by the base current and the component  $J_{g2}$  is increased as a result of this bias. Since the squeezing of the CCR is determined by the component  $J_{g1}$  only, the appearance and increasing of the component  $J_{g2}$  results in the rise of the summary value  $J_g = J_{g1} + J_{g2}$  at the same squeezing. Therefore the efficiency of squeeze control becomes worse. This is a qualitative nature of the influence of the  $n$ -base conductivity which is taken into account in this work.

## 2. EQUATIONS AND TRANSFORMATIONS

The above mentioned system of two equations which describes the distributions of base potentials  $\varphi_p(y)$  and  $\varphi_n(y)$  in the  $p^+npn^+$ -structure can be written in the following form[3]:

$$\frac{d^2\psi_p}{dy^2} = \beta_p^2(e^{\psi_p} + e^{\psi_p - \psi_n}) + \beta_n^2((1 + \gamma_n)e^{\psi_p - \psi_n} - \gamma_n e^{\psi - \psi_n}), \quad (2)$$

$$\xi \frac{d^2\psi_n}{dy^2} = -\beta_n^2(e^{\psi_p - \psi_n} + e^{\psi - \psi_n}) - \beta_p^2((1 + \gamma_p)e^{\psi_p - \psi_n} - \gamma_p e^{\psi_p}), \quad (3)$$

where

$$\psi = e\varphi/T, \quad \psi_{p,n} = e\varphi_{p,n}/T, \quad e^{\psi} = e^{\psi} - 1;$$

$$\beta_p^2 = \frac{e^2 D_n^{(p)} n_0}{\sigma_p T L_p} \operatorname{th} \frac{w_p}{2L_p}, \quad \beta_n^2 = \frac{e^2 D_p^{(n)} p_0}{\sigma_p T L_n} \operatorname{th} \frac{w_n}{2L_n};$$

$$\gamma_p = \frac{\alpha_p}{1 - \alpha_p}, \quad \gamma_n = \frac{\alpha_n}{1 - \alpha_n}. \quad (4)$$

Here  $\alpha_p = 1/ch(w_p/L_p)$ ,  $\alpha_n = 1/ch(w_n/L_n)$  are transport factors of the  $p,n$ -bases,  $\varphi$  is the voltage across the device,  $D_n^{(p)}$  and  $D_p^{(n)}$  are diffusion coefficients of minority carriers (respectively, electrons in the  $p$ -base and holes in the  $n$ -base);  $L_p$ ,  $L_n$  are diffusion lengths and  $p_0$ ,  $n_0$  are equilibrium concentrations of minority carriers,  $T$  is a temperature in energetic units (i.e.  $T = k_B T^*$  where  $k_B$  is Boltzmann's constant and  $T^*$  is a temperature in conventional units which is equal to 300 K for all our calculations). We assume a low-level injection in both bases here.

Equations (2) and (3) have to be solved with boundary conditions:

$$\left[ \frac{d\psi_{p,n}}{dy} \right]_{y=0} = 0, \quad \left[ \frac{d\psi_n}{dy} \right]_{y=1} = 0, \\ \sigma_p \frac{T}{e} \left[ \frac{d\psi_p}{dy} \right]_{y=1} = -J_g. \quad (5)$$

We suppose the currents of both gates are equal in magnitude. The voltage across the device  $\varphi$  is found from a condition of the given anode current

$$J_a = 2 \int_0^l j_a(y) dy \quad (6)$$

or

$$J_a = \frac{2\sigma_p T}{e} \beta_n^2 \int_0^l dy ((1 + \gamma_n) e^{\psi_1 - \psi_n} - \gamma_n e^{\psi_p - \psi_n}).$$

The drawback of the system (2), (3) is that it takes into account only diffusion currents across the *pn*-junctions and neglects generation inside the depletion layers. Therefore this system is correct when diffusion currents predominate over the others overwhelmingly. In particular this takes place in the ON-state when all *pn*-junctions are forward-biased. So we can replace everywhere in eqns (2), (3) and (6)  $e^{\psi_i}$  by  $e^{\psi_i}$ , where  $\psi_i = \psi_p$ ,  $\psi_p - \psi_n$  or  $\psi - \psi_n$ . If the forward voltage across the anode junction 3 is sufficiently large, this approximation is valid when only this junction is forward-biased and two others are reverse-biased.

Let us introduce new dimensionless variables and parameters:  $\eta = y/l$ ,  $\Lambda_a = eJ_a l / 2\sigma_p T$ ,  $\Lambda_g = eJ_g l / \sigma_p T$ ,  $\kappa^2 = \beta_p^2 / \beta_n^2$ . Then instead of eqns (2), (3), (5), (6) we obtain:

$$\frac{d^2 \psi_p}{d\eta^2} = \Lambda_a \frac{\kappa^2 (e^{\psi_p} + e^{\psi_p - \psi_n}) + (1 + \gamma_n) e^{\psi_p - \psi_n} - \gamma_n e^{\psi - \psi_n}}{\int_0^1 d\eta ((1 + \gamma_n) e^{\psi - \psi_n} - \gamma_n e^{\psi_p - \psi_n})}, \quad (7)$$

$$- \xi \frac{d^2 \psi_n}{d\eta^2} = \Lambda_a \frac{\kappa^2 ((1 + \gamma_p) e^{\psi_p - \psi_n} - \gamma_p e^{\psi_p}) + e^{\psi_p - \psi_n} + e^{\psi - \psi_n}}{\int_0^1 d\eta ((1 + \gamma_n) e^{\psi - \psi_n} - \gamma_n e^{\psi_p - \psi_n})}, \quad (8)$$

$$\Lambda_a = (\beta_n l)^2 \int_0^1 d\eta ((1 + \gamma_n) e^{\psi_1 - \psi_n} - \gamma_n e^{\psi_p - \psi_n}), \quad (9)$$

$$\left[ \frac{d\psi_p}{d\eta} \right]_{\eta=1} = -\Lambda_g, \quad \left[ \frac{d\psi_{p,n}}{d\eta} \right]_{\eta=0} = \left[ \frac{d\psi_n}{d\eta} \right]_{\eta=1} = 0. \quad (10)$$

The potentials  $\psi$ ,  $\psi_p(\eta)$ ,  $\psi_n(\eta)$  and dimensionless current densities  $\lambda_a(\eta) = j_a(\eta) / \bar{j}_a$ ,  $\lambda_c(\eta) = j_c(\eta) / \bar{j}_a$  which are determined by these potentials can be specified by giving two current parameters  $\Lambda_a$  and  $\Lambda_g$  and five device parameters  $\gamma_p$ ,  $\gamma_n$ ,  $\xi$ ,  $\kappa^2$ ,  $(\beta_n l)^2$ . (In the above we have introduced a mean anode current density  $\bar{j}_a$ .) If we replace  $e^{\psi_i}$  by  $e^{\psi_i}$  everywhere in the right-hand sides of eqns (7) and (8) (i.e. we neglect thermal generation) we can consider only two variables  $\psi_p(\eta) - \psi$  and  $\psi_n(\eta)$  instead of the three unknown ones  $\psi_p(\eta)$ ,  $\psi_n(\eta)$  and  $\psi$ . Then the condition (9) can be omitted when dimensionless current densities  $\lambda_a(\eta)$  and  $\lambda_c(\eta)$  are sought. These current density distributions depend on four device parameters only:  $\gamma_p$ ,  $\gamma_n$ ,  $\xi$ ,  $\kappa^2$ . (Let us note again that it is correct not only in the case when all three exponen-

tial terms on the right-hand sides of eqns (7) and (8) are large in comparison with 1, but also in the case when only two of them are large:  $\exp(\psi - \psi_n)$ ,  $\exp(\psi_p) \gg 1$  and sometimes it is sufficient  $\exp(\psi - \psi) \gg 1$ ). Therefore it is enough to use only the four above-mentioned parameters in most of actual cases. The parameter  $(\beta_n l)^2$  is required for separation of all potentials.

### 3. PROCEDURES AND APPROXIMATIONS

Systems (7), (8) can be simplified substantially in two limit idealized cases:  $\xi = 0$  and  $\xi = \infty$  which are most convenient for comparison with realistic situations. If  $\xi = 0$  we can equate the right-hand side of eqn (8) to zero and express  $\psi_n$  in terms of  $\psi$  and  $\psi_p$ . After this eqn (7) can be integrated in quadratures. This important particular case was considered in Ref.[3]. When  $\xi = \infty$  we obtain from eqn (8):

$$\psi_n = \text{const}. \quad (11)$$

To calculate this constant we have to use a condition of equality of total currents through the junctions 2 and 3; this is

$$\int_0^1 d\eta (e^{\psi_p - \psi_n} + e^{\psi - \psi_n} + \kappa^2 ((1 + \gamma_p) \times e^{\psi_p - \psi_n} - \gamma_p e^{\psi_p})) = 0. \quad (12)$$

If replacement  $e^{\psi_i} \rightarrow e^{\psi_i}$  is justified we can immediately obtain from eqn (12)

$$e^{-\psi_n} = \frac{\gamma_p \kappa^2 e^{\bar{\psi}_p}}{e^{\bar{\psi}} + (1 + \kappa^2 (1 + \gamma_p)) e^{\bar{\psi}_p}}, \quad (13)$$

where bars over the letters mean averaging over the segment (0, 1). Thus we obtain for  $\xi = \infty$  (as for  $\xi = 0$ ) the single eqn (7), which can be integrated in quadratures.

We are not going to consider integrals of eqn (7) for  $\xi = \infty$  thoroughly, but let us pay attention to a single detail. The anode current density  $\lambda_a(\eta)$  is proportional to

$$(1 + \gamma_n) e^{\psi - \psi_n} - \gamma_n e^{\psi_p - \psi_n}$$

(see an integrand in eqn (9)). The potential difference  $\psi - \psi_n$  is independent of  $\eta$  in this case. So the larger the forward bias of the middle junction 2 (that is  $\psi_p(\eta) - \psi_n$ ), the smaller anode current density  $\lambda_a(\eta)$ . If  $\psi_p(\eta)$  decreases monotonically with  $\eta$ , the current density  $\lambda_a(\eta)$  does not decrease monotonically (as for  $\xi = 0$ ), but on the contrary it increases. That is in the PT-region  $\lambda_a(\eta)$  is greater than in the CCR.

For the arbitrary  $\xi$  we use the following procedure of solution of eqns (7) and (8). Distributions  $\psi_p(\eta, \xi_0)$ ,  $\psi(\xi_0)$  for  $\xi_0 < \xi$  are used as an initial (zero) approximation. They are substituted in the right-hand side of eqn (8), and this equation is integrated numerically with the boundary conditions  $d\psi_n/d\eta|_{\eta=0,1} = 0$ . The new solution  $\psi_n(\eta)$  is substituted in the right-hand side of eqn (7). Numerical

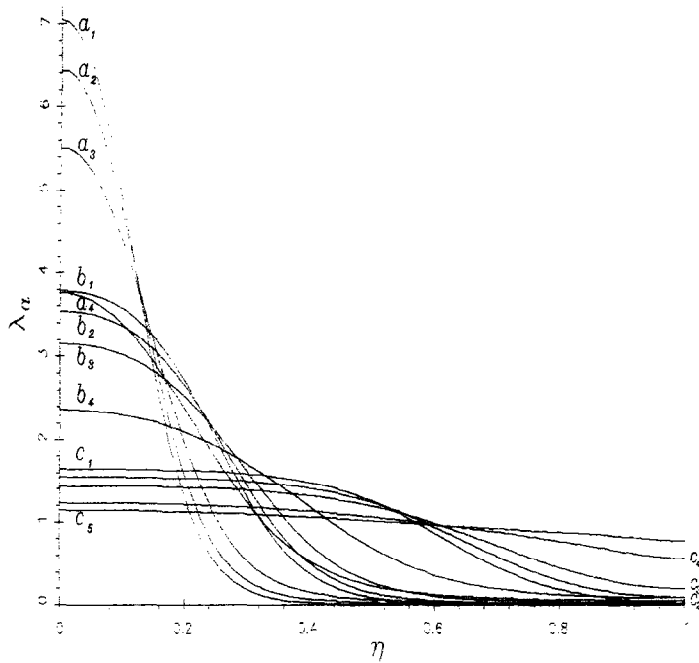


Fig. 2. Anode current distributions  $\lambda_\alpha(\eta)$  for the model A;  $\beta_p l = 1$ ; 1— $\xi = 0$ ; 2— $\xi = 1$ ; 3— $\xi = 3$ ; 4— $\xi = 10$ ; 5— $\xi = 15$ ;  $a_i - \Lambda_g = 32$ ;  $b_i - \Lambda_g = 24$ ;  $c_i - \Lambda_g = 14$ .

integration of it gives the next approximation  $\psi_p(\eta)$ . This self-consistent procedure is repeated until the given precision is achieved. After every integration of eqns (7) or (8),  $\psi$  is corrected according to eqn (9). If  $\xi$  is small ( $\xi < 1$ ), the case  $\xi_0 = 0$  is considered as an initial approximation. But for a large  $\xi$  (and large  $\gamma_n$ ,  $J_g$  in particular) transition from  $\xi_0 = 0$  is required to

be multistage as a rule, that is a few intermediate values of  $\xi_0$  are used. As we can see later, the final distribution deviates from the distribution for  $\xi = 0$  significantly.

Since the main goal of this work is to study the effect of the controlled base conductivity on inhomogeneous distributions of the current densities, we

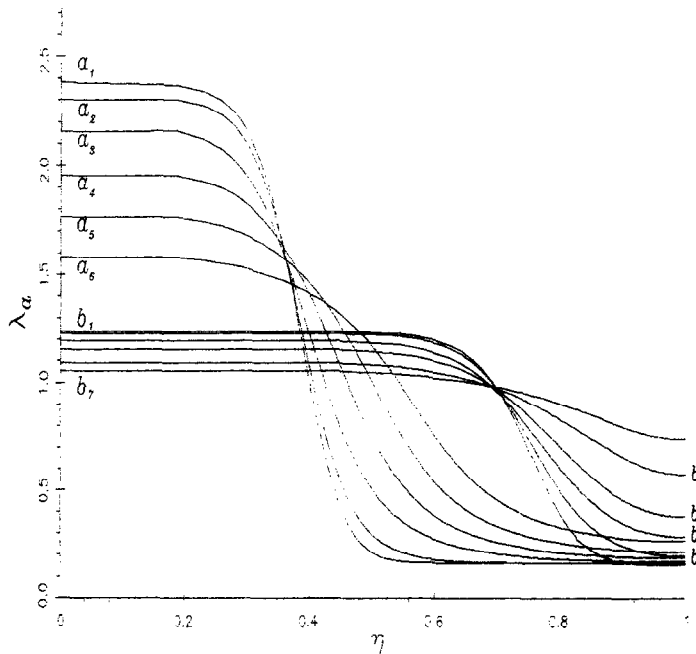


Fig. 3. The same as in Fig. 2 for the model B. 1— $\xi = 0$ ; 2— $\xi = 1$ ; 3— $\xi = 3$ ; 4— $\xi = 5$ ; 5— $\xi = 7$ ; 6— $\xi = 10$ ; 7— $\xi = 15$ ;  $a_i - \Lambda_g = 120$ ;  $b_i - \Lambda_g = 55$ .

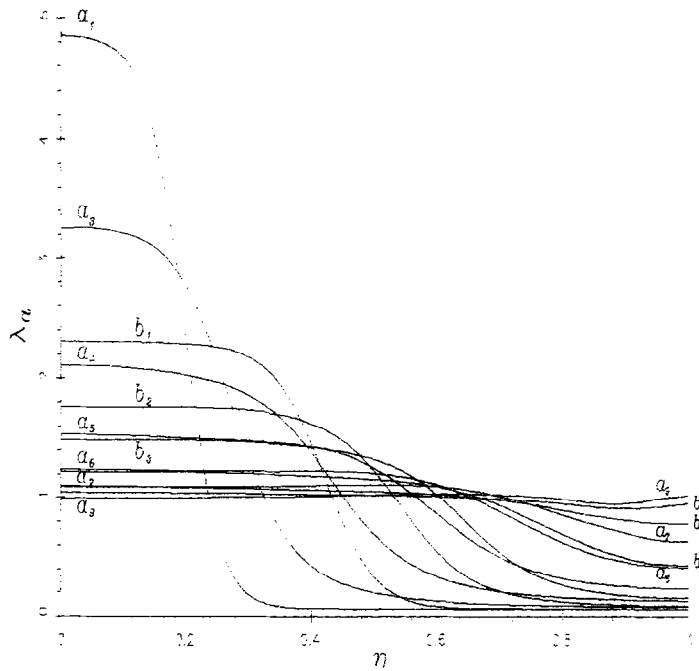


Fig. 4. The same as in Fig. 2 for the model C. 1— $\xi = 0$ ; 2— $\xi = 0.5$ ; 3— $\xi = 1$ ; 4— $\xi = 2$ ; 5— $\xi = 3$ ; 6— $\xi = 4$ ; 7— $\xi = 5$ ; 8— $\xi = 7$ ; 9— $\xi = 10$ ;  $a_i - \Lambda_g = 60$ ;  $b_i - \Lambda_g = 42$ .

present three collections ( $\xi$  from 0 to 10 ÷ 15) of the anode current density distributions for three sets of parameters A, B and C (see Figs 2–4, respectively). Further, these model examples of the device structures are called—“models A, B, C”. Each model is given by a set of parameters  $\gamma_p, \gamma_n, \kappa^2$  (see Table 1). We consider a single value of the current  $\Lambda_a$  for each of them and two of three values of the current  $\Lambda_g$ .  $\Lambda_a$  is selected to demonstrate the effect of gate control clearly and  $\Lambda_g$  corresponds to different stages of the CCR-squeeze. The indirect parameters from Table 1 correspond to the different real parameters of material and structure. As far as the effect of squeezing is of interest for the design of controllable light-emitting devices, we give the examples of such real parameters of *pnpn*- and *nnpn*-structures based on GaAs. Two possible sets of parameters for models A, B, C are given in Table 2. One of these sets relates to *pnpn*-structures with controlling *p*-base and controlled *n*-base (as assumed everywhere in the article) and another relates to *nnpn*-structures with controlling *n*-base and controlled *p*-base which could be more convenient for the design of gate-controlled light-emitting devices. Parameter  $(\beta_p l)^2 = \kappa^2 (\beta_n l)^2$  which determines the contribution of thermal generation currents is equal to 1 in all these cases. It is a very large value. The role of this parameter will be

discussed below. Let us note that the neglect of thermal generation leads to a nonphysical increase of the potential  $\varphi_n(y)$  at large  $y$  (see Ref.[3]).

One can see from Table 1, that  $\kappa^2$  is always assumed to be small. We suppose in all the cases a strong inequality  $\gamma_p \gg \gamma_n$ , that is the controlling base is narrow ( $w_p/L_p < 1$ ) and the controlled base is wide ( $w_n/L_n > 1$ ). Three couples of values  $\gamma_p$  and  $\gamma_n$  provide noticeable variation of the so-called thyristor gate gain  $K_g = \Lambda_a/\Lambda_M(\Lambda_a)$ , where  $\Lambda_M(\Lambda_a)$  designates a maximum value of  $\Lambda_g$ , which maintains state of maximum squeezing of the CCR. Any other exceeding  $\Lambda_g$  over  $\Lambda_M(\Lambda_a)$  causes sharp increase of the voltage across the structure (and the gate turn-off in real circuit conditions).

For  $\xi = 0$  we have

$$K_g = \frac{\gamma_p(1 + \gamma_n)}{\gamma_p\gamma_n - 1} \tag{14}$$

according to the estimate in Ref.[3]. The maximum value of  $K_g = 56$  corresponds to the model A and we see from Fig. 2 that the largest current  $\Lambda_a$  is controlled by smallest values of  $\Lambda_g$ , but large  $K_g$  causes a border broadening of the CCR. An analogous result was obtained in Ref.[3].

Table 1. Set of dimensionless parameters used in the model structures

Model	$\gamma_p$	$w_p/L_p$	$\gamma_n$	$w_n/L_n$	$\kappa^2$	$\Lambda_a$
A	10.0	0.4436	0.12	2.924	0.01	2500.0
B	10.0	0.4436	0.3	2.146	0.01	1000.0
C	3.0	0.7954	1.0	1.317	0.1	500.0

Table 2. Examples of real parameters of material and structure for model structures

	Units	A <i>pnpn</i>	A <i>nprp</i>	B <i>pnpn</i>	B <i>nprp</i>	C <i>pnpn</i>	C <i>nprp</i>
$N_p$	$\text{cm}^{-3}$	$10^{18}$	$10^{18}$	$3 \times 10^{18}$	$10^{17}$	$3 \times 10^{18}$	$3 \times 10^{17}$
$\mu_n^{(p)}$	$\text{cm}^2 \text{V}^{-1} \text{s}^{-1}$	3000	3000	2000	5200	2000	4000
$D_n^{(p)}$	$\text{cm}^2 \text{s}^{-1}$	78	78	52	135	52	104
$\tau_p$	s	$2 \times 10^{-11}$	$8 \times 10^{-11}$	$1.2 \times 10^{-11}$	$10^{-10}$	$1.2 \times 10^{-11}$	$1.2 \times 10^{-10}$
$L_p$	$\mu\text{m}$	0.4	0.8	0.26	1.2	0.26	1.1
$w_p$	$\mu\text{m}$	0.18	2.4	0.12	2.5	0.2	1.4
$\sigma_p$	$10^{-4} \text{Ohm}^{-1}$	5.4	72	7.9	10	13.2	15.4
$N_n$	$\text{cm}^{-3}$	$2 \times 10^{16}$	$10^{18}$	$3 \times 10^{15}$	$10^{18}$	$2 \times 10^{16}$	$10^{18}$
$\mu_p^{(n)}$	$\text{cm}^2 \text{V}^{-1} \text{s}^{-1}$	300	170	350	170	300	170
$D_p^{(n)}$	$\text{cm}^2 \text{s}^{-1}$	7.8	4.4	9.1	4.4	7.8	4.4
$\tau_n$	s	$10^{-9}$	$2 \times 10^{-11}$	$3 \times 10^{-9}$	$2 \times 10^{-11}$	$10^{-9}$	$2 \times 10^{-11}$
$L_n$	$\mu\text{m}$	0.9	0.09	1.6	0.09	0.9	0.09
$w_n$	$\mu\text{m}$	2.6	0.04	3.4	0.04	1.2	0.07
$\sigma_n$	$10^{-4} \text{Ohm}^{-1}$	26	20	10	20	12	36
$\xi$	1	5	3.6	1	0.5	1	0.4

#### 4. RESULTS AND DISCUSSION

Let us consider some conclusions which can be drawn from an analysis of the distributions  $\lambda_a(\eta)$ .

(1) An effect of increasing  $\xi$  consists in a broadening of the border between the CCR and the depletion region (or the PT-region). This border broadens in a direction of the PT especially. The current density in a homogeneous part of the CCR diminishes simultaneously. The cause of the border broadening is an additional current bias of the PT. This current bias causes an increase of the parasitic component of the gate current  $J_{g2}$ . If the total gate current  $J_g = J_{g1} + J_{g2}$  is fixed it leads to decrease of the component  $J_{g1}$  and decrease of the current density in the CCR together with broadening of this region (to save  $J_a = \text{const}$ ).

(2) Increase of  $\xi$  (and therefore the component  $J_{g2}$ ) induces increase of the maximum stationary current  $\Lambda_M(\Lambda_a)$  since the squeeze of the CCR is determined by the component  $J_{g1}$  only.

(3) The greater  $\Lambda_g$  for the given  $\Lambda_a$  the more the effect of the conductivity  $\sigma_n$  and the parameter  $\xi$ . It is due to the superlinear increase of the current density in the quasihomogeneous CCR with  $\Lambda_g$ . (Let us remind ourselves that for  $\xi = 0$ , the current density in this region is proportional to  $J_g^2$ —see Ref.[3]). Therefore, increase of the value  $\Lambda_g$  leads to the faster increase of the current bias of the PT and the component  $J_{g2}$ , respectively. In other words there is a redistribution of the current  $J_g$  between  $J_{g1}$  and  $J_{g2}$  on behalf of  $J_{g2}$ . This causes the more substantial contribution of the controlled base conductivity  $\sigma_n$  for larger values of  $\Lambda_g$ .

(4) The greater  $\gamma_n$  (that is the greater current gain for the common-emitter circuit) the more substantial effect of the parameter  $\xi$  for the same other parameters. That is why the controlled base has to be sufficiently wide and most of the recombination and light emission has to be concentrated in this base.

(5) Figure 5 shows the distributions of the base potentials  $\psi_p(\eta)$  and  $\psi_n(\eta)$  for different values of  $\xi$  in the model A. For  $\xi = 0$ , increase of the potential  $\psi_n$  for increasing  $\eta$  is restricted by the value of floating

potential in the insulated base of the PT. This value is determined by the level of carrier thermal generation in both bases of the structure. The variation of a parameter  $(\beta_p l)^2 = \kappa^2(\beta_n l)^2$  allows us to vary the thermal generation level. This level determines  $\xi$ , which influences the distributions  $\varphi_{p,n}$  and  $\lambda_a(\eta)$  noticeably. The distributions  $\lambda_a(\eta)$  for different  $(\beta_p l)^2$  are shown in Fig. 6.

(6) Most of the distributions  $\lambda_a(\eta)$  demonstrate a monotone decrease with  $\eta$ . Such behaviour is typical for the distributions from Figs 2–4, 6, but some of them demonstrate an increase of  $\lambda_a$  near  $\eta = 1$  (see, for example, curves  $a_9$  and  $b_9$  in Fig. 4). They take place for very large values of  $\xi \geq 10$  and comparatively small  $\Lambda_g$ . This behaviour is a reminder of the above described distribution  $\lambda_a(\eta)$  for  $\xi = \infty$ . In this case we have an increase of  $\lambda_a(\eta)$  near  $\eta = 1$  instead of a monotone decrease.

#### 5. CONCLUSION

The procedure which has been accomplished here is based substantially on assumptions (1). They are satisfied with a large reserve in most of the implemented designs of light-emitting and lasing thyristor-like switches (see, for example Refs[4–8]). Due to the condition (1) we can substantially reduce the two-dimensional problem of carrier concentration and potential distribution in the gate-controlled thyristor-like structure to the system of ordinary differential eqns (2) and (3). The solution of this system for arbitrary values of  $\xi$  is the main difficulty which is surmounted in this work.

We have shown that an increase of the longitudinal conductivity along the controlled base does not influence the CCR squeezing substantially if it does not exceed the conductivity along the controlling base, that is if  $\xi$  does not exceed 1. The value of  $\gamma_n$ , which is determined by the recombination in the controlled base, must not be too large (it must not exceed 1). In all these cases a negative effect of increasing  $\xi$  can be compensated for by an increase of the gate current  $J_g$ .

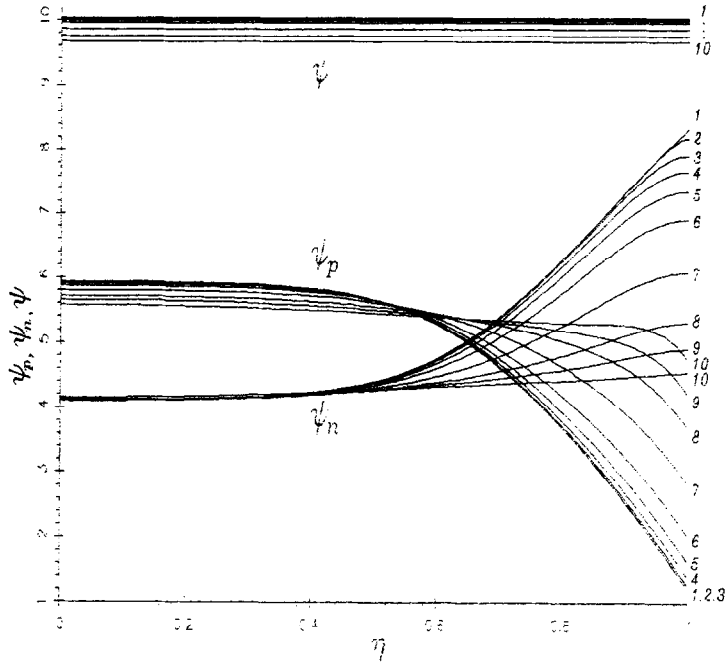


Fig. 5. Distributions of the potentials  $\psi_p$ ,  $\psi_n$  and  $\psi$  for the model A;  $\beta_p l = 1$ ;  $\Lambda_s = 14$ ; 1— $\xi = 0$ ; 2— $\xi = 0.01$ ; 3— $\xi = 0.1$ ; 4— $\xi = 0.25$ ; 5— $\xi = 0.5$ ; 6— $\xi = 1$ ; 7— $\xi = 3$ ; 8— $\xi = 7$ ; 9— $\xi = 10$ ; 10— $\xi = 15$ .

Of course, this compensation decreases the efficiency of the gate control (in the case of gate current modulation of light emission) in comparison with the ideal situation  $\xi = 0$ .

Until now a lot of designs of thyristor-like light-emitting structures have been described in period-

icals. The turn-on and turn-off of light emission in some of them are performed with the help of gate currents in one of the bases[4-7] and even in both bases[8], that is they are gate-controlled light switches. Evidently the above described RITO can be realized in each of these devices. In this regime,

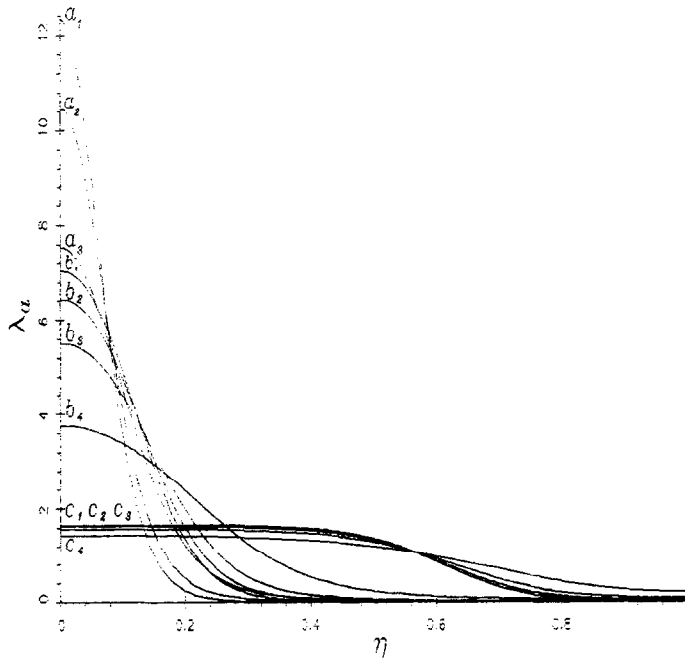


Fig. 6. The same as in Fig. 2 for the model A with  $\Lambda_s = 32$  and different values of  $\beta_p l$ ; 1— $\xi = 0$ ; 2— $\xi = 1$ ; 3— $\xi = 3$ ; 4— $\xi = 10$ ;  $a_i$ — $\beta_p l = 0.5$ ;  $b_i$ — $\beta_p l = 1$ ;  $c_i$ — $\beta_p l = 2$ .

light-emission is controlled by the gate current. The opportunity to turn on and off laser generation in the laser diodes with the help of the gate current variation only could be very important.

An experimental implementation of the RITO for light-emitting thyristor-like structures could accomplish effective double modulation, which is very attractive both in the incoherent light-emitting devices and in laser diodes especially[9].

The above presented results are the first ones in this field and therefore they are not free from a number of simplifying assumptions. Of course for a more detailed theory we need to reject the low-level injection assumption (especially in the controlled *n*-bases). Taking into account the applied nature of the effect, one has to turn from calculations of *pnpn*-homostructures to heterostructures, since all modern light-emitting devices are heterostructural ones. In the above, we use assumptions (1) which allow us to simplify the calculations. But these assumptions being valid for all implemented realizations of light-emitting thyristor-like switches are apparently not optimum. It will probably be necessary to use substantially two-dimensional numerical calculations (similar to the ones that are only justified in power GTO-thyristors—see, for example Refs[10,11]).

*Acknowledgements*—The authors thank the Ukrainian Foundation of Fundamental Researches for partial support of this work.

#### REFERENCES

1. Z. Gribnikov and A. Rothwarf, *Solid-St. Electron.* **37**, 135 (1994).
2. Z. Gribnikov, V. Mitin and A. Rothwarf, *Proc. of 1993 ISDRS*, Vol. 2, p. 603 (1993).
3. N. Z. Vagidov, Z. S. Gribnikov, A. N. Korshak and V. V. Mitin, *Fiz. Tekh. Poluprovodn.* **29**, 1958 (1995) (in English: *Semiconductors* **29**, 102 (1995)).
4. G. W. Taylor, R. S. Mand, J. G. Simmons and A. Y. Cho, *Appl. Phys. Lett.* **50**, 338 (1987).
5. D. L. Crawford, G. W. Taylor and J. G. Simmons, *Appl. Phys. Lett.* **52**, 863 (1988).
6. D. L. Crawford, G. W. Taylor, P. W. Cooke, T. Y. Chang, B. Tell and J. G. Simmons, *Appl. Phys. Lett.* **53**, 1797 (1988).
7. P. R. Claisse, G. W. Taylor, D. P. Docter and P. W. Cooke, *IEEE Trans. Electron Devices* **ED-39**, 2523 (1992).
8. K. Kasahara, Y. Tashiro, N. Hamao, M. Sugimoto and T. Yanase, *Appl. Phys. Lett.* **52**, 679 (1988).
9. V. B. Gorfinkel and S. Luryi, *Appl. Phys. Lett.* **62**, 2923 (1993).
10. A. Nakagawa and D. H. Navon, *IEEE Trans. Electron Devices* **ED-31**, 1156 (1984).
11. A. Nakagawa, *Solid-St. Electron.* **28**, 677 (1985).